Tunnelling and Underground Space Technology 65 (2017) 140–154

Contents lists available at ScienceDirect

Tunnelling and Underground Space Technology

journal homepage: www.elsevier.com/locate/tust

A case study of TBM performance prediction using a Chinese rock mass classification system – Hydropower Classification (HC) method

Quansheng Liu [a,b], Jianping Liu [a,c,*], Yucong Pan [a,c], Xiaoxuan Kong [b], Kairong Hong [d]

[a] State Key Laboratory of Geomechanics and Geotechnical Engineering, Institute of Rock and Soil Mechanics, Chinese Academy of Sciences, Wuhan, Hubei 430071, PR China
[b] Key Laboratory of Safety for Geotechnical and Structural Engineering of Hubei Province, School of Civil Engineering, Wuhan University, Wuhan, Hubei 430072, PR China
[c] University of Chinese Academy of Sciences, Beijing 100049, PR China
[d] State Key Laboratory of Shield Machine and Boring Technology, Zhengzhou, Henan 450001, PR China

ARTICLE INFO

Article history:
Received 17 April 2016
Received in revised form 18 November 2016
Accepted 6 March 2017
Available online 17 March 2017

Keywords:
Hydropower Classification method
Tunnel boring machine (TBM)
Performance prediction
Field penetration index (*FPI*)

ABSTRACT

Basic Quality (BQ) method is a basic national standard of rock mass classification suitable for different industries in geomechanics and geotechnical engineering in China. Referring to the relevant provisions of BQ method, Hydropower Classification (HC) method, a specialized engineering geological classification system widely used in China, was compiled for evaluation on overall stability of surrounding rock and guide of excavation and support design of underground engineering in water conservancy and hydropower industry. As the input parameters of BQ or HC method are quite different with those used in RMR or Q system, which indirectly limits the applicability of the foreign developed TBM performance prediction models for the China's TBM tunnelling projects. In order to develop an empirical model for hard rock TBM performance prediction with more suitable applicability in China, 49 valid datasets were collected from a water conveyance tunnel mostly excavated in medium to hard igneous rocks, and the empirical relationships between TBM performance and each parameter in the database were studied. The results showed that the prediction accuracies of TBM performance based on *HC* or *BQ* are very limited as the effects of the input parameters of HC method on field penetration index (*FPI*) are different and their weights assigned are improper. TBM penetration rate (*PR*) reaches its maximum value in the *HC* range 40–60 and *BQ* range 350–450, respectively. Boreability of the rock mass in class III is higher than that in class II. Ridge regression, principal component regression and partial least-squares regression methods were employed to solve the multicollinearity between uniaxial compressive strength of intact saturated rock, intactness index of rock mass, angle between discontinuity plane and tunnel axis, and average overburden of tunnel section in the database. Comparisons between the measured *FPI* and predicted *FPI* showed good agreement. This highlights the powerful potential of multiple regression analysis model based on HC method in TBM performance prediction. However, it deserves to emphasize that the developed empirical relationships should be considered valid only for new projects with geological conditions similar to the studied tunnel in this study, and more field data from different projects need to be collected to develop a universal model in the future.

© 2017 Elsevier Ltd. All rights reserved.

1. Introduction

With the rapid development of modernization in China, hard rock tunnel projects of various diameters, lengths and overburdens are being widely constructed in water conservancy and hydropower, transportation, mining and other industries. China has already been the country with the fastest development speed, largest construction scale and highest construction difficulty of tunnel excavation in the world currently. As stated by Reilly et al. (2002): "mechanized tunnel excavation and advanced underground construction technologies are regarded as one new field of the 21st century by the western countries, so it can generally be named the century of tunnel engineering". Tunnel boring machine (TBM) has been widely used in hard rock tunnelling for its fast advance rate, high excavation quality, favorable environmental protection, low labor intensity (Qian and Li, 2002). By incorporating the latest technological achievements in mechanical, hydraulic, optical and electrical engineering, TBM has been updated to a large scale and high technical tunnel construction equipment that can

* Corresponding author at: State Key Laboratory of Geomechanics and Geotechnical Engineering, Institute of Rock and Soil Mechanics, Chinese Academy of Sciences, Wuhan, Hubei 430071, PR China.

E-mail address: jpliu_whrsm@foxmail.com (J. Liu).

http://dx.doi.org/10.1016/j.tust.2017.03.002
0886-7798/© 2017 Elsevier Ltd. All rights reserved.

conduct tunnelling, mucking, guiding and supporting simultaneously. Since its first successful employment in 1990s, more than 50 tunnels have been completed in China so far through absorbing the accumulated experience of TBM tunnelling projects in the past 50 years in western countries. According to the related statistics, tunnels with total length more than 4000 km will be constructed by about 130 TBMs in the next 10 years in China (Liu et al., 2016a). Pelizza et al. (2002) indicated that, with the largest construction scale never encountered by western countries, the Western China Development will provide a unique opportunity for the implementation of TBM tunnelling method.

With high sensitivity to varying geological conditions and enormous financial investment in initial project phase, accurate prediction of TBM performance with respect to special ground conditions has a crucial importance for arranging construction schedule and assessing excavation cost. However, it is always quite difficult to reveal the genuine correlation between TBM performance and rock mass properties deeply due to the extremely complex interaction mechanism of rock-machine. In the past three decades, a large number of TBM performance prediction models have been developed and these models can be generally divided into two main categories, i.e. theoretical and empirical ones (Rostami et al., 1996). Based on rock fragmentation mechanism, theoretical models, e.g. CSM model (Rostami, 1997), analyze the cutting forces acting on individual disc cutter to obtain the force equilibrium equations through indentation tests or full-scale linear cutting tests (Roxborough and Phillips, 1975; Snowdon et al., 1982; Sanio, 1985; Rostami and Ozdemir, 1993; Rostami, 1997). As the theoretical models are limited by the available test facilities and the effects of joint conditions on the cutting process are not considered, empirical formulas based on field data are more convenient to master by constructors, and thus widely developed and preferred in TBM performance prediction (Tarkoy, 1973; Graham, 1976; Blindheim, 1979; Farmer and Glossop, 1980; Nelson et al., 1983, 1985; Bamford, 1984; Hughes, 1986; Wijk, 1992; Sundin and Wänstedt, 1994; Laughton, 1998; Bruland, 1998; Alvarez Grima et al., 2000; Ribacchi and Lembo-Fazio, 2005; Yagiz, 2008; Gong and Zhao, 2009; Hassanpour et al., 2009, 2010, 2011). Empirical models have been improved from simple ones to complex ones. The early simple empirical models which are no longer used for their low prediction accuracy only considered a few intact rock mechanical properties, e.g. compressive strength, tensile strength and hardness. With accessibility to more TBM construction data, several complex empirical models have been established by researches using multiple regression analysis, fuzzy mathematics, neural network and so on, and NTNU model (Bruland, 1998) is the best known one. Prediction accuracy of the complex empirical models depends largely on the similarity degree of the ground conditions, machine specifications and operation parameters between the target tunnel and the original database, and higher similarity degree generally leads to more accurate prediction results. At present, TBM performance prediction models for specific geological conditions are still rarely developed, e.g. mixed grounds (Steingrimsson et al., 2002; Zhao et al., 2007; Tóth et al., 2013), grounds with toxic gases (Shahriar et al., 2009), blocky rock conditions (Delisio et al., 2013, Delisio and Zhao, 2014), highly fractured and faulted rock conditions (Paltrinieri et al., 2016), thus deeper investigation and research about these specific ground conditions need to be conducted in the future.

Comparing with more than 30 TBM performance prediction models available in foreign published literatures, only two simple empirical models are reported by Chinese researchers (Song et al., 2008; Du et al., 2015). TBM performance is the comprehensive interaction result between the machine and excavated rock mass. Liu et al. (2016b) counted the using frequency of rock mass properties and machine parameters in total 17 models, including theoretical models and complex empirical models, and found that the using frequency of rock mass properties decreased in the order of discontinuity spacing (15 times, including *RQD*, J_v, J_s and *CFF*), intact rock uniaxial compressive strength (12 times), angle between the discontinuity and the tunnel axial (6 times), tunnel diameter (5 times), rock brittleness (4 times, including *PSI* and S_{20}) and so on, and the using frequency of machine parameters decreased in the order of equivalent thrust per cutter (8 times), revolutions per minute (4 times), cutter diameter (3 times), cutter spacing (2 times), cutter tip width (1 time) and angle of the contact area between rock and disc cutter (1 time).

As most of the rock mass properties used for TBM performance prediction are related to the input parameters of rock mass classification systems, some researchers attempt to link TBM performance with these systems (Cassinelli et al., 1982; Innaurato et al., 1991; Mcfeat-Smith and Askilsrud, 1993; Grandori et al., 1995; Palmström, 1995; Sundaram and Rafek, 1998; Barton, 1999; Alber, 2000; Sapigni et al., 2002; Ribacchi and Lembo-Fazio, 2005; Bieniawski et al., 2006, 2007a, 2007b, 2008; Bieniawski and Grandori, 2007; Hassanpour et al., 2009, 2010, 2011; Hamidi et al., 2010). However, the input parameters of RMR (Bieniawski, 1989) or Q system (Barton et al., 1974) are quite different with those used in BQ (The National Standards Compilation Group of People's Republic of China, 2014) or HC method (The National Standards Compilation Group of People's Republic of China, 2009), the two commonly used rock mass classification systems in China, which indirectly limits the applicability of the foreign developed TBM performance prediction models for the China's TBM tunnelling projects. Therefore, this study attempts to develop an empirical model for hard rock TBM performance prediction based on multiple regression analysis of HC method.

2. Basic Quality (BQ) method and Hydropower Classification (HC) method

Standard for engineering classification of rock masses (GB/T50218-2014), BQ method for short, provides one necessary and fundamental basis for the exploration, design, and quota compilation of rock engineering construction. It combines both the qualitative and quantitative methods to determine the basic quality of rock mass, and then takes the characteristics of the specific engineering into account to obtain the rock mass classification (The National Standards Compilation Group of People's Republic of China, 2014). Considering the extremely complex nature of rock mass, compilation of such a basic national standard is the first attempt for different industries in geomechanics and geotechnical engineering in the world. The reliability of BQ method has been verified in water conservancy and hydropower, transportation, railway, and mining projects since it was implemented in China (Wu and Liu, 2012). *BQ* is determined in accordance with two basic factors, namely intact rock strength and rock mass intactness degree, and can be calculated using Eq. (1) (The National Standards Compilation Group of People's Republic of China, 2014):

$$BQ = 90 + 3 * R_c + 250 * K_v \tag{1}$$

where *BQ* is the rock mass rating of BQ method, R_c is the uniaxial compressive strength of intact saturated rock (MPa), K_v is the intactness index of rock mass.

It deserves to emphasize that two restricted conditions should be obeyed when using Eq. (1), i.e. 1. Substituting $R_c = 90 * K_v + 30$ and K_v into Eq. (1) to obtain *BQ* when $R_c > 90 * K_v + 30$; 2. Substituting $K_v = 0.04 * R_c + 0.4$ and R_c into Eq. (1) to obtain *BQ* when $K_v > 0.04 * R_c + 0.4$. The corresponding rock mass classification of BQ method is shown in Table 1.

Table 1
Rock mass classification based on BQ method.

BQ	>550	550–451	450–351	350–251	≤250
Classification	I	II	III	IV	V

Considering the industry characteristics of the rock engineering construction and application, water conservancy and hydropower industry, on the basis of the relevant provisions of BQ method, compiled an engineering geological classification system, i.e. HC method, to evaluate overall stability of surrounding rock and guide excavation and support design of underground engineering. The reliability of HC method has been verified in many hydropower stations constructed in China, such as three gorges, xiangjiaba, xiluodu, wudongde and baihetan (Shen et al., 2014). Intact rock strength, rock mass intactness degree, and discontinuity conditions are regarded as the basic influence factors in HC method, and all of them are assigned with positive values. Moreover, groundwater condition and attitude of the major discontinuity plane are employed as correction factors in HC method and assigned with negative values. A composite index, namely the cumulative score T, is deduced based on the above mentioned five factors using the accumulation method and can be calculated using Eq. (2) (The National Standards Compilation Group of People's Republic of China, 2009):

$$T = A + B + C + D + E \tag{2}$$

where T is the rock mass rating of HC method, A, B, C, D, E are the ratings of rock strength, rock mass intactness degree, discontinuity conditions, groundwater condition and the main discontinuity plane attitude, respectively.

Meanwhile, rock mass classification is synthetically determined by taking the strength-stress ratio S into consideration to involve the effect of stress state on the stability of surrounding rock. The strength-stress ratio S can be calculated using Eq. (3) (The National Standards Compilation Group of People's Republic of China, 2009):

$$S = \frac{R_c * K_v}{\sigma_m} \tag{3}$$

where S is the strength-stress ratio, σ_m is the maximum principal stress of surrounding rock (MPa), which could be replaced with geostatic stress when no measured information is obtained in the field.

The corresponding rating criterion of each input parameter and rock mass classification of HC method are shown in Tables 2–7 (The National Standards Compilation Group of People's Republic of China, 2009) respectively.

3. Project description and database development

3.1. Project and geology

The data used for TBM performance analysis in this study were collected from a water conveyance tunnel mostly excavated in medium to hard igneous rocks. This project includes two main tunnels constructed with TBM tunnelling method and one middle connection tunnel excavated with drill and blast method. The database established in excavating the first main tunnel was employed in this study. The main geomorphic types of this tunnel are erosional landforms with either tectonic or accumulational movements. Under the influence of regional tectonic movements, the faults encountered along the tunnel are mainly compressive and compressive-shear types with the major strike direction NE. The major fault crossed by the tunnel is F65 with relatively larger scale and effect over other smaller faults. In-situ investigation shows that the main lithologies along the tunnel are Cretaceous adamellite, Jurassic granodiorite, and Permian monzogranite, as shown in Fig. 1. Overburden of the whole tunnel axis varies from 120 to 300 m, maximum to 424 m, and the longitudinal slope along the advance direction is 0.3115‰. Tunnel diameters before and after lining are 8.53 and 7.60 m, respectively. Based on field exploration data and at least 6 groups of laboratory test results of preconstruction phase, the main physical and mechanical properties of the rocks are shown in Table 8.

3.2. TBM specifications and tunnelling operation

A gripper TBM, as shown in Fig. 2, manufactured cooperatively by Northern Heavy Industries Group Company Limited and Robbins Company, was employed in this project. The cutterhead is laced with 49 disc cutters, including 4 double-ring center cutters with 17 in. or 432 mm, 37 single-ring face cutters with 20 in. or 508 mm and 8 single-ring gauge cutters with 20 in. or 508 mm. Other main technical parameters of the TBM are summarized in Table 9. The TBM commenced excavation in January 2014 and by December 2014 the tunnel of 5.234 km was completed. Statistical analyses show that the average and highest monthly advances are 436.17 m and 956.25 m, respectively, and the average and highest monthly utilization rates are 37.5% and 49.5%, respectively.

3.3. Database development

There are two field data collection approaches in developing empirical models for TBM performance prediction, one is to select the average values of the target parameters in a tunnel section with relatively longer length, and the other is to choose the instantaneous values of the target parameters in a tunnel section with relatively shorter length. If data accuracy can be surely guaranteed, then both of the two methods are alternative. In this study, the second method was selected for the TBM operation parameters change frequently.

As an important part of engineering construction, geological work needs to be conducted simultaneously during TBM tunnelling. The main tasks of geological work that needs undertaken

Table 2
Rock strength rating of HC method.

Rock strength type	Hard rock		Soft rock	
	Strong rock	Moderately hard rock	Relatively soft rock	Weak rock
Uniaxial compressive strength of intact saturated rock R_c (MPa)	$R_c > 60$	$60 \ge R_c > 30$	$30 \ge R_c > 15$	$15 \ge R_c > 5$
Rock strength rating *A*	30–20	20–10	10–5	5–0

Note: 1. A is assigned with 30 points when R_c exceeds 100 MPa; 2. If the total ratings of B and C is less than 5 points, A is assigned with 20 points when A is larger than 20 points.

Table 3
Rock mass intactness degree rating of HC method.

Rock mass intactness degree		Integrated	Relatively integrated	Poorly integrated	Relatively fractured	Fractured
Intactness index of rock mass K_v		$K_v > 0.75$	$0.75 \geq K_v > 0.55$	$0.55 \geq K_v > 0.35$	$0.35 \geq K_v > 0.15$	$K_v \leq 0.15$
Rock mass intactness degree rating B	Hard rock	40–30	30–22	22–14	14–6	<6
	Soft rock	25–19	19–14	14–9	9–4	<4

Note: 1. If R_c is in the range of 30–60 MPa, the total ratings of B and C is assigned with 65 points when that is larger than 65 points; 2. If R_c is in the range of 15–30 MPa, the total ratings of B and C is assigned with 55 points when that is larger than 55 points; 3. If R_c is in the range of 5–15 MPa, the total ratings of B and C is assigned with 40 points when that is larger than 40 points; 4. If R_c is less than 5 MPa, the ratings of B and C are assigned with 0 point respectively.

Table 4
Discontinuity conditions rating of HC method.

Discontinuity conditions	Width (mm)	Close $W < 0.5$		Slightly open $0.5 \leq W < 5.0$									Open $W \geq 5.0$	
	Filler	–		None			Debris			Mud			Debris	Mud
	Shape	Wa. and Ro.	St. and Sm.	Wa. and Ro.	Wa. and Sm. or St. and Ro.	St. and Sm.	Wa. and Ro.	Wa. and Sm. or St. and Ro.	St. and Sm.	Wa. and Ro.	Wa. and Sm. or St. and Ro.	St. and Sm.	–	–
Discontinuity conditions rating C	Hard rock	27	21	24	21	15	21	17	12	15	12	9	12	6
	Relatively soft rock	27	21	24	21	15	21	17	12	15	12	9	12	6
	Weak rock	18	14	17	14	8	14	11	8	10	8	6	8	4

Where Wa. represents waviness, Ro. represents roughness, St. represents straightness and Sm. represents smoothness. Note: 1. When the length of discontinuity is shorter than 3 m, extra 3 points and 2 points are added into C of hard rock, relatively soft rock and weak rock respectively, and when the length of discontinuity is longer than 10 m, extra 3 points and 2 points are subtracted from C of hard rock, relatively soft rock and weak rock respectively; 2. When the width of discontinuity without filler is larger than 10 mm, C is assigned with 0 point.

Table 5
Groundwater condition rating of HC method.

Groundwater condition			Dripping or seepage state	Linear-flow state	Water-inrush state
Water quantity q (L/min * 10 m) or pressure head H (m)			$q \leq 25$ or $H \leq 10$	$25 < q \leq 125$ or $10 < H \leq 100$	$q > 125$ or $H > 100$
Basic factor rating T'	$T' > 85$	Groundwater condition rating D	0	0 to −2	−2 to −6
	$85 \geq T' > 65$		0 to −2	−2 to −6	−6 to −10
	$65 \geq T' > 45$		−2 to −6	−6 to −10	−10 to −14
	$45 \geq T' > 25$		−6 to −10	−10 to −14	−14 to −18
	$T' \leq 25$		−10 to −14	−14 to −18	−18 to −20

Note: 1. Basic factor rating T' is the total ratings of A, B and C, namely $T' = A + B + C$; 2. D is assigned with 0 point for dryness state.

Table 6
The main discontinuity plane attitude rating of HC method.

Angle between discontinuity plane strike and tunnel axis β (°)		90–60°				60–30°				<30°			
Discontinuity plane dip α_f (°)		>70°	70–45°	45–20°	≤20°	>70°	70–45°	45–20°	≤20°	>70°	70–45°	45–20°	≤20°
The main discontinuity plane attitude rating E	Roof	0	−2	−5	−10	−2	−5	−10	−12	−5	−10	−12	−12
	Sidewall	−2	−5	−2	0	−5	−10	−2	0	−10	−12	−5	0

Note: When rock mass intactness degree belongs to poorly integrated, relatively fractured or fractured, E is assigned with 0 point.

Table 7
Rock mass classification based on HC method.

Class	Cumulative score T	Strength-stress ratio S
I	$T > 85$	>4
II	$85 \geq T > 65$	>4
III	$65 \geq T > 45$	>2
IV	$45 \geq T > 25$	>2
V	$T \leq 25$	–

Note: When the strength-stress ratio S of rock mass in class I, II, III and IV is less than the specified value in Table 7, rock mass classification should be reduced by one grade.

throughout the whole construction process include advance geological forecast, surrounding rock quality evaluation and rock mass classification. During TBM tunnelling, tunnel section with approximate uniform rock mass classification is regarded as one engineering geological unit, and if the rock mass classification changes remarkably, then the logging work on the next engineering geological unit will start automatically. The length of the engineering geological unit in this study is about 32 m, which approximately equals to the distance from shield tail to the shotcrete robot. The main contents of geological logging include:

- Logging of the name, color, and weathering degree of surrounding rock, etc.
- Determination of the intact rock strength and rock mass intactness degree.
- Logging of the position, scale, attitude and fillings of faults or joints, etc.
- Logging of the position and dimensions of fallen-blocks and local collapses, etc.
- Logging of the construction method, excavation rate and the size of the representative mucks.
- Logging of the tunnel temperature.

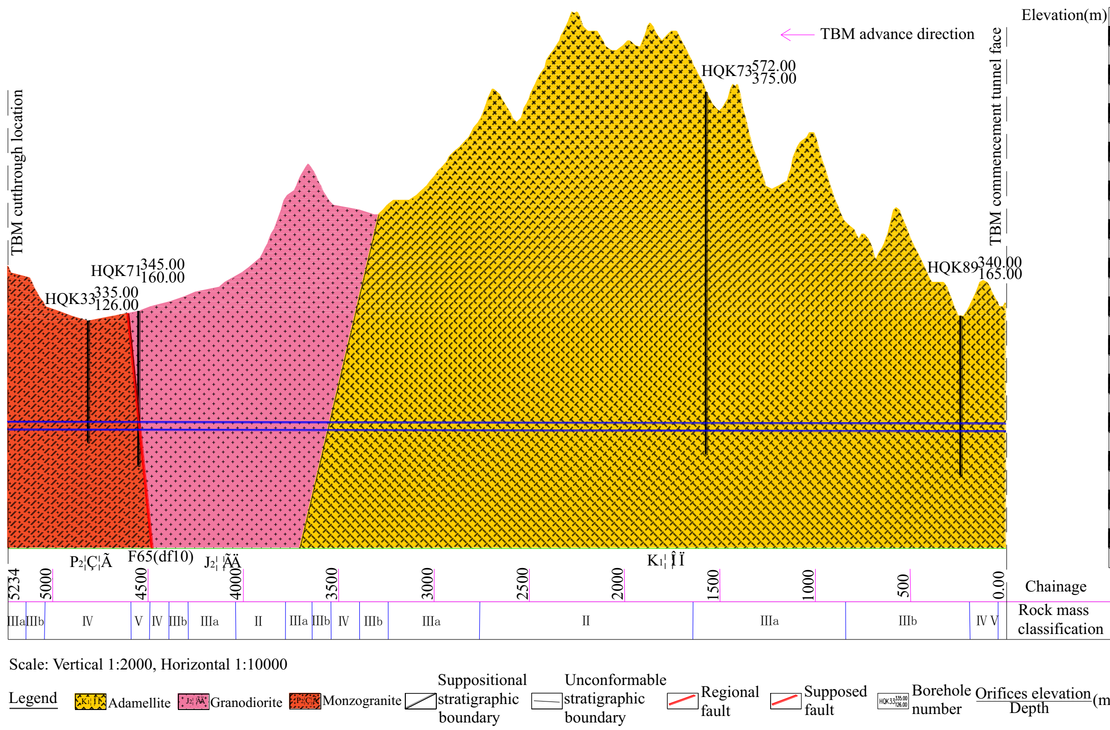

Fig. 1. Geological section along the tunnel.

Table 8
Main physical and mechanical properties of the rocks.

Strata code	Rock type	Dry density (g/cm^3)	Natural density (g/cm^3)	Saturated density (g/cm^3)	Specific gravity	Natural water absorption (%)	Saturated water absorption (%)	UCS		P-wave velocity (m/s)
								Dry (Mpa)	Saturated (Mpa)	
P2ηγ	Monzogranite	2.66	2.68	2.69	2.74	1.18	1.24	50–80	50–70	6200
J2γδ	Granodiorite	2.73	2.73	2.74	2.74	0.25	0.29	70–85	60–75	6200
K1ξo	Adamellite	2.64	2.65	2.66	2.68	0.38	0.53	70–80	60–70	6200

Fig. 2. Gripper TBM employed in this study.

(1) Uniaxial compressive strength of intact saturated rock

To characterize the water-softening property of surrounding rock, uniaxial compressive strength of the intact saturated rock

Table 9
Main technical parameters of the TBM.

Technical parameter	Design value
Machine diameter (m)	8.5
TBM model	Robbins MB280
TBM type	Open
Individual cutter nominal load (kN)	311.5
Average face cutter spacing (mm)	89
Cutterhead power (kW)	10 × 330 = 3300
Rotational speed (rpm)	0–5.5
Cutterhead nominal torque	9633 (@0–3.3 rpm) 5695 (@5.5 rpm)
Cutterhead nominal thrust (kN)	16509.5
Maximum allowable thrust (kN)	18,769 at 345 bar
Thrust cylinder stroke (m)	1.8
Conveyor capacity (t/h)	2196
TBM weight (tons)	Approx. 825
Total TBM weight (tons)	Approx. 1375

was adopted as the quantitative index of rock strength (The National Standards Compilation Group of People's Republic of China, 2014). Because of the inconvenient rock coring procedure from tunnel face or tunnel wall to undertaking standard laboratory rock mechanical tests, point load test, for its portable testing apparatus and uncritical sample-size requirement, was selected in this study to indirectly determine the uniaxial compressive strength of intact saturated rock in site. Besides, the result of point load test is more representative in reflecting the full-face rock strength characteristics to some extent for its random sampling. Ribacchi and Lembo-Fazio (2005) also declared that the strength index obtained from point load test is more representative of the failure mechanism of rock under the loading of cutters of TBM.

20 irregular lumps, conformable to the requirement of point load test, were selected randomly from the muck-site or the temporary muck-site under the emergency belt. The lumps were saturated by water immersion in a vacuum of less than 800 Pa (6 torr) for a period of at least 1 h, with periodic agitation to remove trapped air (Franklin, 1979), and the corrected $I_{s(50)}$ of each irregular lump was determined in accordance with the ISRM standard (Franklin, 1985). Two highest and two lowest values of the corrected $I_{s(50)}$, with total number not less than fifteen, were deleted and the average value of the remaining $I_{s(50)}$ values was used to represent the point load strength index of the corresponding tunnel section. Then uniaxial compressive strength of the intact saturated rock can be calculated using Eq. (4) (The National Standards Compilation Group of People's Republic of China, 2014):

$$R_c = 22.82 * I_{s(50)}^{0.75} \tag{4}$$

where $I_{s(50)}$ is the corrected point load strength index of rock sample with 50 mm diameter (MPa).

(2) Intactness index of rock mass

The p-wave velocity in the fractured rock mass is slower to some extent for the existence of discontinuity planes and filling materials. The initial and decreased p-wave velocity can reflect the physical and mechanical properties of either the intact rock block or the fractured rock mass, respectively. Thus, intactness index of rock mass indicates both the development degree and existing conditions of the discontinuity planes, and is a comprehensive index reflecting intactness degree of rock mass (The National Standards Compilation Group of People's Republic of China, 2014). Therefore, BQ and HC methods both regard intactness index of rock mass as the main quantitative index in characterizing the intactness degree of the fractured rock mass. Generally, the p-wave velocity in the rock mass can be measured through different acoustic test methods, including single-hole method, cross-hole method and hammering method. Since drilling direction can significantly affect the measured p-wave velocity in the fractured rock mass, cross-hole method was preferred in this study to obtain the p-wave velocity of the representative area in each engineering geological unit along the tunnel axis. In this study, the requirements for the drill holes in the tunnel wall are as follows:

- Depth and dip angle of the two drill holes should be 5–6 m and 4–5°, respectively.
- Horizontal distance between the two drill holes should be 2–5 m.
- Diameter of the two holes should be no less than 50 mm, and the wall of the two holes should be smooth.

Any muck or powder remained in the two holes is not permissible.

- The two drill holes should be parallel to each other.

The p-wave velocity in intact rock can be determined using the proposed value in Table 8 or the measured value of the representative rock core, and then intactness index of rock mass can be calculated using Eq. (5) (The National Standards Compilation Group of People's Republic of China, 2014):

$$K_v = \left(\frac{V_{pm}}{V_{pr}}\right)^2 \tag{5}$$

where V_{pm} is the p-wave velocity in rock mass (m/s), and V_{pr} is the p-wave velocity in intact rock (m/s).

(3) Discontinuity conditions

The discontinuity conditions include the length, width, filler and shape of the discontinuity plane. Generally, the rating of the discontinuity conditions in an engineering geological unit depends on the major discontinuity plane, referring to the one with the weakest strength that controls the stability of surrounding rock. Geological mapping of the tunnel wall, including discontinuity conditions logging, was conducted during the daily maintenance of the machine.

(4) Groundwater condition

Four categories of groundwater condition used in this study are dryness, dripping or seepage, linear-flow and water-inrush. The groundwater condition was simultaneously recorded during the tunnel wall geological mapping.

(5) Attitude of the major discontinuity plane

The attitude of discontinuity plane mainly includes the dip of the discontinuity plane and the angle between the strike of the discontinuity plane and tunnel axis. The rating of the discontinuity attitude on the roof and sidewall should be separately conducted for the underground projects with long-span and high sidewalls. Similarly, the discontinuity attitude was recorded during the tunnel wall geological mapping.

It is a well-known fact that the major discontinuity plane with limited length cannot fully represent the detailed characteristics of all existing discontinuity planes in an engineering geological unit. Thus the rock mass classification at different positions in the same engineering geological unit will be slightly different, and they should be subdivided to ensure the accuracy of the collected data. Therefore, the major discontinuity plane, where cross-hole acoustic test was undertaken, was selected to determine the rock mass classification of the corresponding tunnel section.

The influence of the angle between the discontinuity plane and tunnel axis on TBM performance has been widely reported by many researches (Aeberli and Wanner, 1978; Lislerud, 1988; Bruland, 1998; Gong et al., 2005; Gong and Zhao, 2009; Hamidi et al., 2010; Ma and Ji, 2011; Mo et al., 2012; Zou et al., 2012; Bejari and Hamidi, 2013; Tan et al., 2013; Kong et al., 2015). Therefore, the discontinuity plane which affects the TBM tunnelling to the most extent, namely joint set with the highest frequency or the minimum spacing was selected, and the angle between the discontinuity plane and tunnel axis can be calculated using Eq. (6) suggested by Bruland (1998):

$$\alpha = \arcsin(\sin\alpha_f * \sin(\alpha_t - \alpha_s)) \tag{6}$$

where α is the angle between the discontinuity plane and tunnel axis (°), α_f and α_s are the dip and strike of the discontinuity plane (°), and α_t is the tunnel axis direction (°).

(6) In situ stress

It is rarely possible to successionally measure the in situ stress along the tunnel in the field. Therefore, combining with the preliminary exploration result, average overburden of each tunnel section was adopted to characterize the in situ stress state on the tunnel face, as conducted by Hamidi et al. (2010).

(7) Machine parameters

The machine parameters, including thrust of the hydro-cylinder, torque, revolution per minute, penetration per revolution, motor current and advance distance, were recorded automatically by an on-board acquisition and recording system. The machine parameters, where p-wave velocity test in the rock mass was undertaken, were employed to represent the TBM performance.

(8) Rock mass boreability

Rock mass boreability is an important indicator to evaluate rock mass fragmentation efficiency and a passive response parameter of rock mass under the loading process of TBM. Boreability can be defined as the resistance (in terms of ease or difficulty) encountered by a TBM as it penetrates a rock mass composed of intact rock and discontinuities (Bruland, 1998). The commonly used rock mass boreability evaluation indices include penetration rate (*PR*), penetration per revolution (*PRev*), field penetration index (*FPI*) (Hamilton and Dollinger, 1979), specific penetration (*SP*, inverse of *FPI*) (Wanner and Aeberli, 1979), fracturing factor (k_s) (Bruland, 1998) and specific rock mass boreability index (*SRMBI*) (Gong et al., 2007). Among the above indices, *FPI* has been widely and successfully applied to evaluate the rock mass boreability (Hassanpour et al., 2009, 2010, 2011; Hamidi et al., 2010; Delisio et al., 2013, Delisio and Zhao, 2014; Du et al., 2015). The advantage of *FPI* is elimination the effect of two major TBM operational parameters including equivalent thrust per cutter and penetration per revolution, and the disadvantage of *FPI* is that it cannot reflect the nonlinear relationship of $F_n/PRev$ (Laughton, 1998; Farrokh et al., 2012). Only when *PRev* exceeds the threshold value (1 mm/rev), then the relationship between $F_n/PRev$ can be roughly considered approximately linear, and thus acceptable results can be obtained (Hamidi et al., 2010). Therefore, *FPI* was employed to evaluate rock mass boreability in this study. The smaller *FPI* is, the higher rock mass boreability will be.

The total thrust offered by the hydro-cylinder is not entirely acting on the tunnel face for gripper TBM, and the efficient thrust is the projection of the total thrust along the advance direction and needs to overcome the friction force between the shield and surrounding rock. Delisio and Zhao (2014) suggested that it is prudent to subtract about 20% weight of the main machine out of the total thrust to account for friction force. Therefore, the friction force in this study was calculated as about 1650 kN. *FPI* can be calculated using Eq. (7):

$$FPI = \frac{F_n}{PRev} = \frac{T * \sin\beta - f}{N * PRev} \tag{7}$$

where *FPI* is the field penetration index (kN/cutter/mm/rev), F_n is the equivalent thrust per cutter (kN/cutter), ignoring the different loading situations of the center cutter, face cutter and gage cutter, *PRev* is the penetration per revolution (mm/rev), *T* is the total thrust of the hydro-cylinder (kN), *f* is the friction force between the shield and surrounding rock, *N* is the number of the rings installed on the cutterhead, β is the angle between the thrust cylinder and the gripper cylinder (°), which reaches its maximum value when the elongation of the thrust cylinder reaches a stroke, the range of β is from 69° to 75° for the TBM in this study, the average value 72° was adopted for subsequent calculation.

In order to ensure the data accuracy, the established database was filtrated based on the following criterions:

– Exclude the datasets obtained from the engineering geological units with abnormal geological structures, e.g. fault and fractured zones, intrusions.
– Exclude the datasets obtained from the engineering geological units changing distinctly in rock type, weathering degree and other factors.
– Exclude the datasets obtained from the engineering geological units without sufficient backup information.
– Exclude the datasets obtained in the first two months considering the influence of learning effect and machine debugging process.

The database employed for TBM performance analysis consists of 49 datasets from 49 tunnel sections after the data filtration process, containing the input parameters and their ratings in HC method, the angle between the discontinuity plane and tunnel axis (α), the average overburden of tunnel section (*H*), the rock mass ratings of HC method (*HC*) and BQ method (*BQ*), the measured TBM performance parameters including penetration rate (*PR*) and field penetration index (*FPI*). The descriptive statistics of the variables in the database is summarized in Table 10.

4. Empirical relationships development

4.1. Relationships between TBM performance and different parameters

Rock strength is one of the important parameters affecting TBM performance, which significantly influences the size and shape of the crushed zone and the initiation and propagation modes of the cracks during the indentation of a cutter. The correlations between R_c and its rating *A* with *FPI* illustrated in Fig. 3 present strong linear relationships. Moreover, the determination coefficient of R_c and *FPI* is larger compared with that of *A* and *FPI*. The main reason is that *A* was assigned with 30 points when R_c exceeds 100 MPa (see Table 2), and obviously, such rating assignation is not applicable for evaluating TBM performance. A simple example is that the excavation of rock mass with R_c = 100 MPa is much easy than that of rock mass with R_c = 200 MPa and the same other input parameters of HC method.

Intactness degree of rock mass, which can affect the initiation and propagation modes of the cracks and the chipping and spalling of the chips, is another important parameter influencing TBM performance. Fig. 4 shows the linear correlations with both R^2 = 0.570 between K_v and its rating *B* with *FPI*, respectively. It should be noted that *B* is related to the rock strength (see Table 3). Fortunately, the rock strength type in the filtrated database is all hard rock, so *B* is equal to 40 times of the K_v value. Therefore, the determination coefficient of K_v and *FPI* is the same as that of *B* and *FPI*.

Consideration of discontinuity conditions is an important characteristic of HC method different from BQ method. It has been proven that homogeneous assumption for the rock mass is not appropriate for stability analysis of the underground engineering (The National Standards Compilation Group of People's Republic of China, 2009). The influence of discontinuity conditions on TBM performance has seldom been reported currently. The weak correlation with R^2 = 0.152 between the discontinuity conditions rating *C* and *FPI* is illustrated in Fig. 5. Two reasons can account for this conclusion that seems contradictory with the result of Hamidi et al. (2010). On the one hand, discontinuity conditions are qualitative indices affected by human factors to some degree. On the other hand, *C* is closely related to the rock strength in HC method (see Table 4). Further studies are needed to reveal the inherent correlation between discontinuity conditions and TBM performance.

The maximum weights assigned to the three basic factors, i.e. rock strength, rock mass intactness degree and discontinuity conditions, are 0.3, 0.4 and 0.3 in HC method, respectively. However, the determination coefficients of the three basic factors with *FPI*

Table 10
Descriptive statistics of the variables in the database.

Parameter	Sample number	Range	Minimum	Maximum	Mean	Std. deviation
R_c (MPa)	49	70.2	45.4	115.6	78.261	18.1655
A	49	14.9	15.1	30.0	24.239	4.3014
K_v	49	0.67	0.17	0.84	0.5853	0.16877
B	49	26.8	6.8	33.6	23.412	6.7509
C	49	18	9	27	18.27	4.720
GW	49	1	1	2	1.24	0.434
D	49	6.7	−6.7	0.0	−1.153	2.1547
α (°)	49	58.7	18.4	77.1	44.957	12.6728
E	49	10	−10	0	−2.41	2.999
H (m)	49	291.0	109.9	400.9	205.233	84.8950
HC	49	52.4	35.0	87.4	62.355	13.5172
BQ	49	312.0	268.4	580.4	465.655	88.7515
PR (m/h)	49	2.80	1.60	4.40	2.6776	0.66435
FPI (kN/cutter/mm/rev)	49	74.82	11.86	86.68	40.3278	21.14105

Note: GW = groundwater condition, where 1 represents dryness state, 2 represents dripping or seepage state, 3 represents linear-flow state and 4 represents water-inrush state.

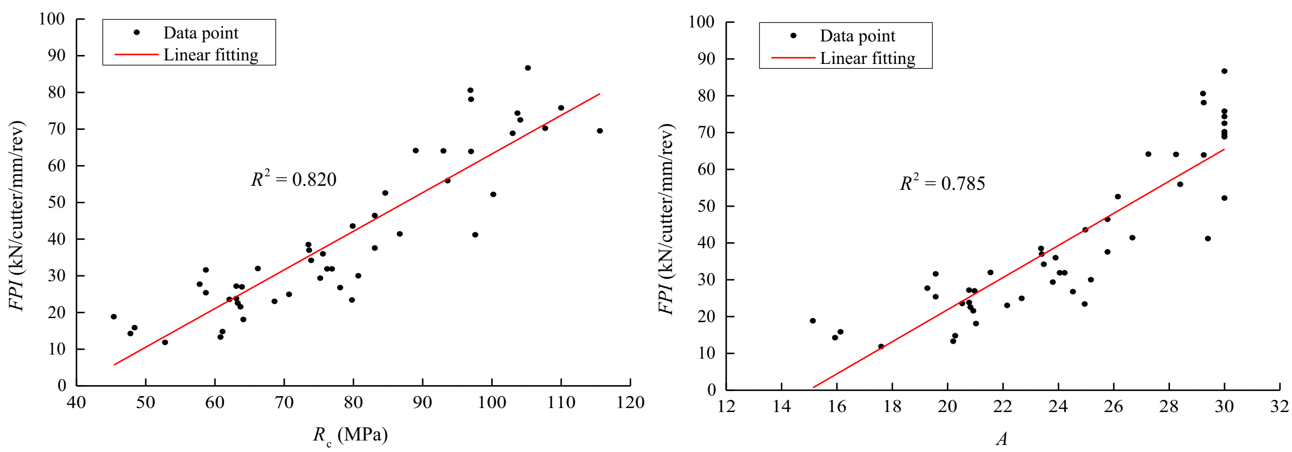

(a) R_c and *FPI*. **(b)** A and *FPI*

Fig. 3. Relationships between R_c and its rating A with *FPI*.

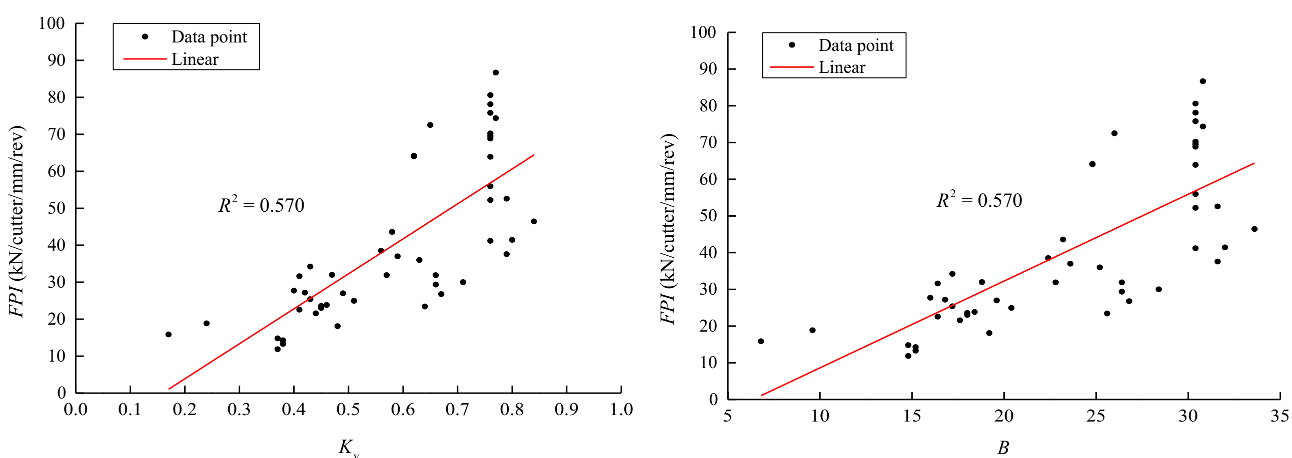

(a) K_v and *FPI*. **(b)** B and *FPI*

Fig. 4. Relationships between K_v and its rating B with *FPI*.

in this study are 0.785, 0.570 and 0.152, respectively, which clearly demonstrates the rating assignation of HC method is not suitable for TBM performance prediction.

Groundwater condition is one of the environmental factors greatly affecting the stability of surrounding rock. The accidents of surrounding rock instability are generally accompanied with groundwater inflow. Groundwater condition also is a qualitative index and its rating D relates to the basic factor rating T'. The weak correlation with $R^2 = 0.268$ between groundwater condition and *FPI* is illustrated in Fig. 6. Attention should be paid for that approx-

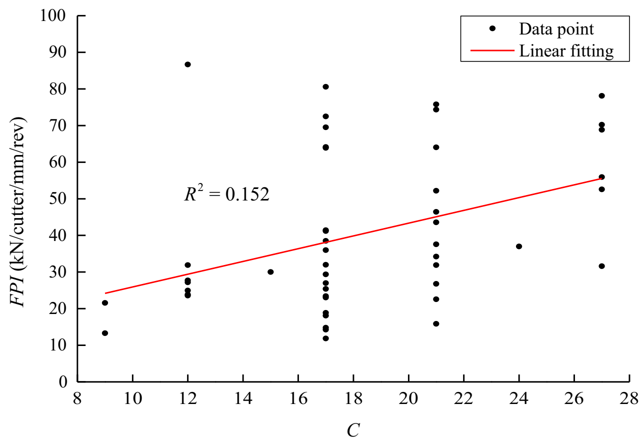

Fig. 5. Relationship between discontinuity conditions rating *C* and *FPI*.

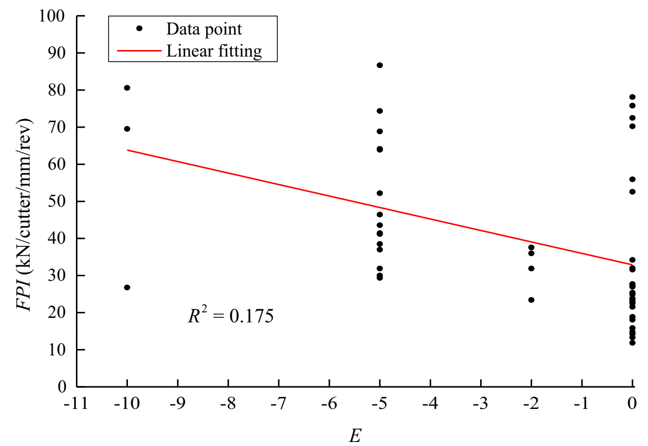

Fig. 7. Relationship between the main discontinuity plane attitude rating *E* and *FPI*.

imately 80% of the data points were obtained in dryness cases and the remaining 20% in dripping or seepage cases, and none valid data points of linear-flow and water-inrush cases were recorded in the database, therefore, the reliability of this conclusion remains further validation for its relatively narrow distribution range of groundwater condition. Now, it is generally accepted that the groundwater condition mainly impacts advance rate rather than penetration rate (Laughton, 1998; Hamidi et al., 2010). Hassanpour et al. (2010) stated that groundwater has an indirect effect on the machine performance with increasing alteration of the rock mass and decreasing strength parameters of the intact rock and joint surface condition. Hamidi et al. (2010) proposed that the groundwater flow in rock mass decreases the rock brittleness, consequently decreases the penetration rate. The meaningless correlation between *FPI* and groundwater condition may be described via this counterbalanced effect of water flow in rock mass.

Attitude of the major discontinuity plane is a correction factor in HC method. Considering the tunnel size and the main support position in this study, attitude of the major discontinuity plane is generally investigated and rated for the roof surrounding rock. Fig. 7 shows the weak linear correlation with $R^2 = 0.175$ between the main discontinuity plane attitude rating *E* and *FPI*. This is mainly because that *E* is obtained based on the influence degree of the major discontinuity plane attitude on the stability of the roof surrounding rock, not directly relevant to the rock mass boreability. The correlation between α angle and *FPI* is illustrated in Fig. 8. As seen in Fig. 8, rock mass boreability reaches optimum in the α angle range 40–55°, which agrees well with the empirical finding obtained by Hamidi et al. (2010). Many researches (Bruland, 1998; Gong et al., 2005; Gong and Zhao, 2009; Ma and Ji, 2011; Mo et al., 2012; Zou et al., 2012; Bejari and Hamidi, 2013; Tan et al., 2013; Kong et al., 2015) have indicated that the best α angle for TBM tunnelling is around 60° in rock mass with large joint spacing (approximately 100 mm or larger), and the best α angle transforms from 60° to 90° with the decrease of joint spacing. It should be noted that the best α angle is relevant to the selected evaluation index of rock mass boreability. In addition, the relationship with $R^2 = 0.237$ between α angle and *FPI* is not good as expected. On the one hand, the weak correlation may result from that 69% data points concentrate on the narrow range 30–50°. On the other hand, the widths of the discontinuity planes partial are slightly open or entirely close, and the geological compass is interfered by the complicated magnetic field in site, hence, attitude of the major discontinuity plane is empirically evaluated by geological engineers and affected by their engineering practices. As stated by Ramezanzadeh (2005): "finding a reasonable relationship between discontinuity orientation alone and TBM parameters is not easy".

In situ stress is another environmental factor affecting the stability of surrounding rock. Influences of in situ stress on rock cutting process and TBM performance are not yet completely investigated and revealed in available literatures. However, it is generally believed that in situ stress not only affects TBM penetration rate but also TBM advance rate. Several studies based on three-dimensional confined indentation results noted that the significant indentation force increase at higher confinement levels (Kaitkay and Lei, 2005; Yin et al., 2014), however, two-dimensional indentation

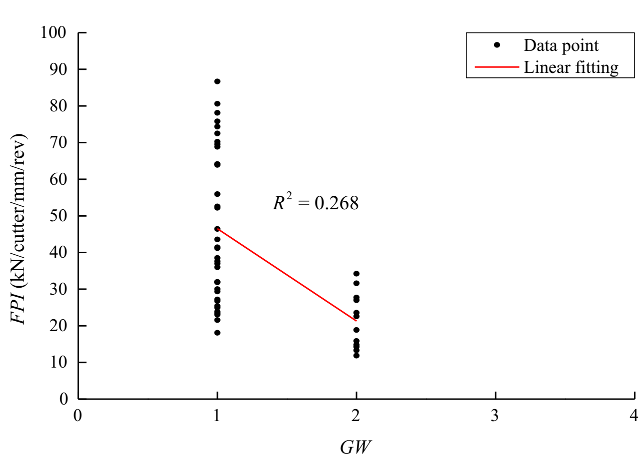

Fig. 6. Relationship between groundwater condition and *FPI*.

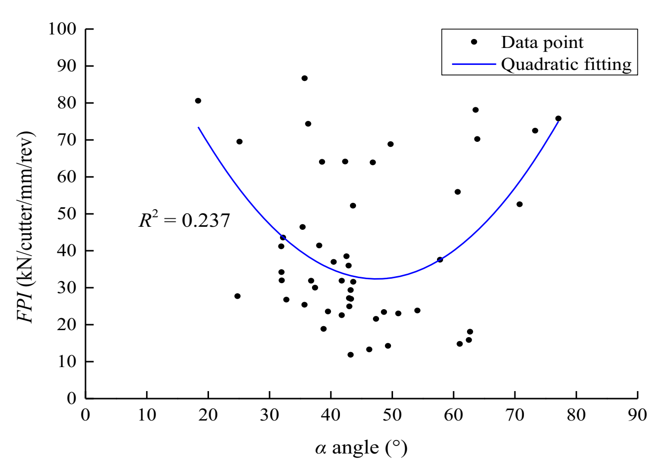

Fig. 8. Relationship between alpha angle and *FPI*.

tests conducted by Huang et al. (1998), Chen and Labuz (2006) and Innaurato et al. (2007) revealed that the limited influence of increasing confining stress on the indentation pressure. Meanwhile, it is a general known fact that confining stress would change the rock failure mode and decrease the rock cuttability. Confined indentation tests clearly showed the failure mode transition from brittle to ductile at higher confining stress (Chen and Labuz, 2006; Ma et al., 2011), and the rock drillability decreases by almost 30% when highly stressed (Innaurato et al., 2007). However, some studies also demonstrated that the long median crack will gradually go upwards into lateral directions forming chips with the increase of confining stress (Chen and Labuz, 2006; Ma et al., 2011), and thus some certain confined cases will facilitate rock fragmentation for rock slabbing induced by confining stress may occur before TBM cutter indentation (Wu et al., 2010; Gong et al., 2010; Yin et al., 2014). And when in situ stress is very high and rock is overstressed, slabbing and spalling, face overbroken and ground squeezing may occur, which will greatly affect the penetration rate and advance rate in a negative sense (Gong et al., 2012). Different opinions with respect to the influences of confining stress on TBM excavation can largely attribute to the different rock strength properties and confining stress levels.

The correlation between the average overburden of tunnel section *H* and *FPI*, shown in Fig. 9, indicates that *FPI* increases with increased *H*, implying that rock mass boreability decreases with higher tunnel overburden as expected. The determination coefficient of *H* and *FPI* with $R^2 = 0.555$ in this study is much larger than that of the result obtained by Hamidi et al. (2010). This is mainly because that the average tunnel overburden for nearly 85% of the datasets used in their study is in the narrow range of 50–200 m, and the average tunnel overburden in this study is relatively uniformly distributed from 100 to 400 m, thus the result is more credible.

4.2. Relationships between TBM performance and surrounding rock ratings

The input parameters of different rock mass classifications vary from each other to some extent, but the development purposes of them all are to evaluate overall stability of surrounding rock and guide excavation and support design of underground engineering. Thus, statistical analyses show that there are significant correlations between different rock mass classification systems. The empirical relationships of *RMR* and *BQ* (Wu and Liu, 2012), *Q* and *RMR* (Bieniawski, 1989), *RSR* and *RMR* (Bieniawski, 1989), *GSI* and *RMR* (Hoek and Brown, 1997) are shown as follows, respectively:

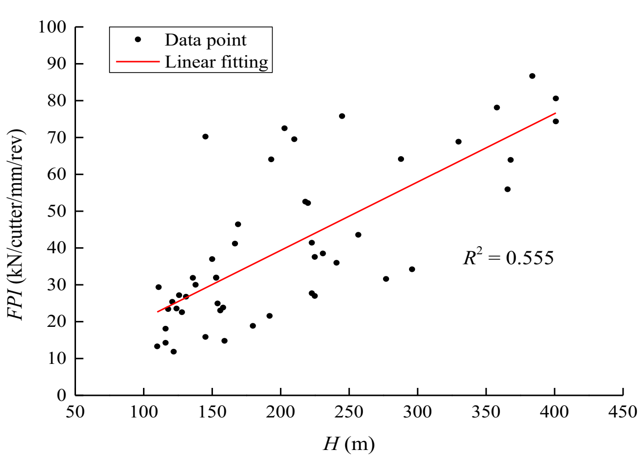

Fig. 9. Relationship between average overburden of tunnel section *H* and *FPI*.

$$RMR = (BQ - 80.79)/6.09 \quad (8)$$

$$Q = EXP((RMR - 44)/9) \quad (9)$$

$$RSR = 0.77RMR + 12.4 \quad (10)$$

$$GSI = RMR - 5 \quad (11)$$

where *RMR* is the rating of RMR system, *Q* is the rating of Q system, *RSR* is the rating of RSR system, and *GSI* is the rating of GSI system.

The empirical relationships between TBM performance and surrounding rock ratings were studied based on the 49 valid datasets. Fig. 10 illustrates the correlations between *PR* with *HC* and *BQ*. As shown in Fig. 10, the scatter range is rather wide, and the TBM penetration rate is fitted with *HC* and *BQ* by a quadratic curve more closely than that by a linear trend. TBM penetration rate reaches its maximum value in the *HC* range 40–60 and *BQ* range 350–450, respectively. Slower penetration rates will be experienced in both too bad and too good rock masses, consistent with the results of Sapigni et al. (2002) and Hamidi et al. (2010). This attributes to that in order to avoid premature damage and excessive wear of the disc cutters resulting from machine vibration and damage, TBM operators tend to reduce the total thrust of the hydro-cylinder when tunnelling in weak rock mass accompanied with face instability, mucking and gripping problems, thus the TBM penetration rate decreases. However, due to the high strength of intact rock or the good intactness degree of rock mass, the capacities of cutter indentation and crush, crack initiation and propagation, chip chipping and spalling are somehow restricted and thus reduced in very good rock mass, and consequently slower penetration rates are obtained.

The correlations between *FPI* with *HC* and *BQ*, illustrated in Fig. 11, show that the distribution of the collected data is also scattered. The quadratic polynomial relationship is superior over the linear relationship for *FPI* and *BQ*, however, similar for *FPI* and *HC*. Moreover, boreability of the rock mass in class III is higher than that in class II because *FPI* tends to decrease with the degradation of surrounding rock rating. Meanwhile, *FPI* remains nearly constant for the rock mass in class IV, which is consistent with the result obtained by Hamidi et al. (2010). The main reason attributes to that the intactness degree of the rock mass in class IV is generally poor, thus TBM operators will reduce the total thrust normally, as previously mentioned, and descending degree of the equivalent thrust per cutter nearly equals to that of penetration per revolution resulted from lower TBM *PR*. Therefore consequently, *FPI* remains unchanged for the rock mass in class IV.

In addition, it can be found in Figs. 10 and 11 that the determination coefficients of the *BQ* with *PR* and *FPI* are both larger than those of the *HC* with *PR* and *FPI*. This may result from that BQ method only considers the effects of uniaxial compressive strength of intact saturated rock and intactness index of rock mass on the stability of surrounding rock, however, the influences of discontinuity conditions, groundwater condition and attitude of the major discontinuity plane on the stability of surrounding rock are taken into account in HC method besides the two above factors.

4.3. Development of empirical models for TBM performance prediction based on HC method

TBM performance, as the result of multiple-factor interaction in rock excavation process, not only relates to the properties of intact rock and rock mass, but also connects with the design and operation parameters of TBM. Multiple regression analysis method has been widely used in exploring the potential relationship between the single dependent variable and many independent variables. A

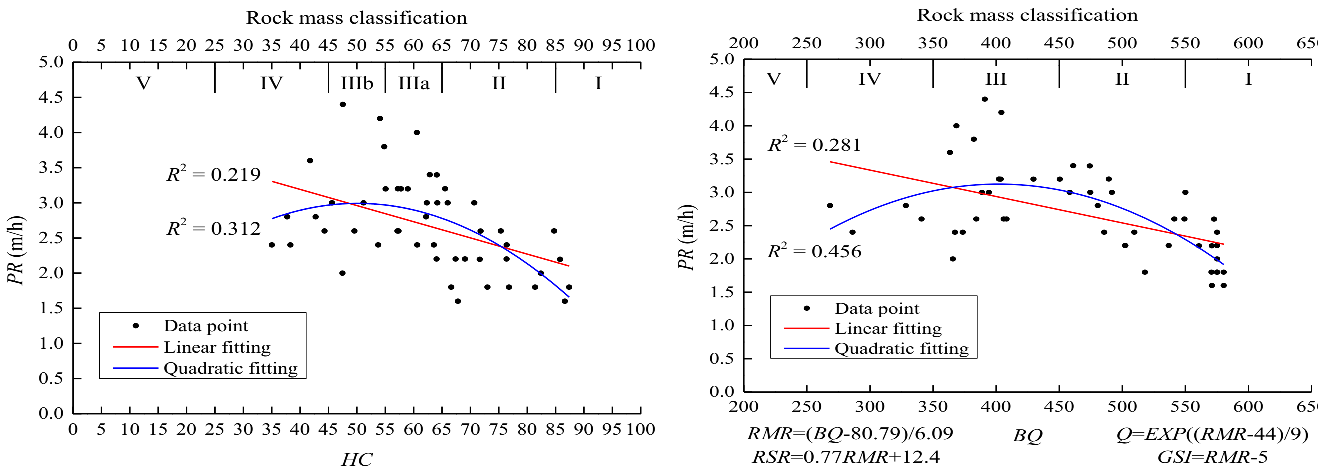

(a) *HC* and *PR*. **(b)** *BQ* and *PR*.

Fig. 10. Relationships between surrounding rock ratings and *PR*.

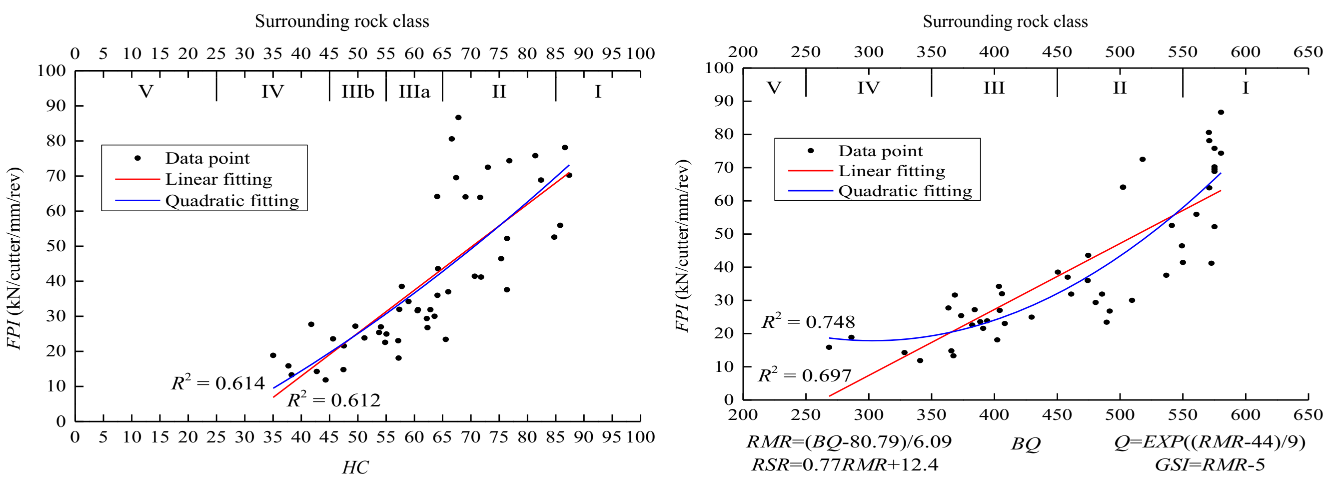

(a) *HC* and *FPI*. **(b)** *BQ* and *FPI*.

Fig. 11. Relationships between surrounding rock ratings and *FPI*.

professional statistical analysis software (SPSS) was employed in this study for predicting TBM performance accurately.

Based on the above analyses, the discontinuity conditions, groundwater condition and attitude of the major discontinuity plane are excluded from the list of independent variables used for the multiple regression analyses for their weak correlations with *FPI*, and this is also why the determination coefficients of *BQ* with *PR* and *FPI* are both larger than those of *HC* with *PR* and *FPI*. Four parameters, i.e. R_c, K_v, α, and H were selected for developing empirical TBM performance prediction models. After a series of modeling, the *FPI* prediction model obtained from multiple linear regression is as follows:

$$FPI = -45.290 + 1.001R_c - 20.780K_v + 1.284\ \mathrm{Log}\ \alpha + 0.085H(R_a^2 = 0.898) \quad (12)$$

where R_a^2 is the adjusted determination coefficient.

As can be seen in Eq. (12), the coefficient sign of intactness index of rock mass (K_v) is negative, which runs counter to the professional judgment that higher rock mass intactness degree leads to lower rock mass boreability. In this case, it is necessary to check for any types of multicollinearity between the independent variables used in the regression model. Multicollinearity means that linear relationships exist between the independent variables, i.e., an independent variable can be expressed with a linear function of other one or more independent variables. If multicollinearity exists, then the least-squares method will be invalid, the coefficient estimation will be damaged, the model error will be expanded, and the model robustness will be lost at the same time (Wang, 1999). The existence of multicollinearity can be determined by observing the correlation coefficient matrix of the independent variables, shown in Table 11. Strong correlation coefficient with $R = 0.883$ between R_c and K_v is shown in Fig. 12, which is easily conceivable. R_c and K_v are basic characteristics of rock mass and rarely depend on project types. Hamidi et al. (2010) stated that most regressions have some degree of multicollinearity due to the nature of observational data. The multicollinearity problem can be solved effectively using ridge regression, principal component regression and partial least-squares regression methods.

Ridge regression, an improved least-squares method, is a biased estimation regression method special for the analysis of multicollinearitied data. In order to obtain an equation with more credible regression coefficients, ridge regression gives up the unbiasedness of the least-squares method at the cost of losing some information

Table 11
Correlation coefficient matrix between the independent variables.

Correlation coefficient	R_c	K_v	Log α	H
R_c	1.000	0.883	0.054	0.564
K_v	0.883	1.000	−0.004	0.475
Log α	0.054	−0.004	1.000	−0.074
H	0.564	0.475	−0.074	1.000

and reducing the accuracy. The residual standard deviation of the ridge regression is greater than that of the least-squares regression, but the tolerance ability for the pathological data of the former is far stronger than that of the latter (Zhang and Dong, 2013). Using ridge regression method, the ridge trace curves become stable when the ridge parameter (k) is greater than 0.30. Therefore, 0.30 is assigned to k, and the ridge regression model is as follows after converting the standardized independent variables into the original ones:

$$FPI = -34.892 + 0.521R_c + 19.907K_v + 3.868\ \mathrm{Log}\ \alpha + 0.080H(R_a^2 = 0.853) \tag{13}$$

Principal component regression conducts the regression analysis process using the principal components of the original independent variables instead of themselves. The former ones contain the majority information of the original independent variables and are unrelated to each other. Therefore, regression coefficients based on the least-squares model using principal components can generally avoid the multicollinearity problem (Zhang and Dong, 2013). Two principal components with the characteristic root greater than 1.00, of which the cumulative variance contribution ratio reaches 82.889%, were selected. Eventually, the established principal component regression model is as follows:

$$FPI = -42.149 + 0.443R_c + 46.010K_v + 3.583\ \mathrm{Log}\ \alpha + 0.073H(R_a^2 = 0.834) \tag{14}$$

The partial least-squares method is a new multiple statistical analysis method, which can provide much richer information besides a more reasonable regression model. In short, the basic principle of least-squares method is to minimize the cumulative longitudinal distance of all data points to the regression line, but the basic principle of partial least-squares method is to minimize the cumulative vertical distance of all data points to the regression line (Zhang and Dong, 2013). Compared with classical multiple regression analysis method, partial least-squares method has many advantages (Wang, 1999):

- Obtain a regression model even serious multicollinearity problem exists between the independent variables.
- Allow to establish models even sample number less than the variable number.
- Identify the system information and noise easily, even some random noise.

The regression model based on partial least-squares regression method is as follows:

$$FPI = -61.958 + 0.590R_c + 14.980K_v + 15.062\ \mathrm{Log}\ \alpha + 0.1107H(R_a^2 = 0.873) \tag{15}$$

The F-tests related to the utility of the overall regression models of ridge regression, principal component regression and partial least-squares regression were carried out. The statistic value F and *Sig.* of the three models are 70.527, 121.585, 166.200 and 0, 4.3339E−19, 0, respectively. Therefore, the null hypothesis can be rejected. That means at least one of the independent variables can significantly affect FPI.

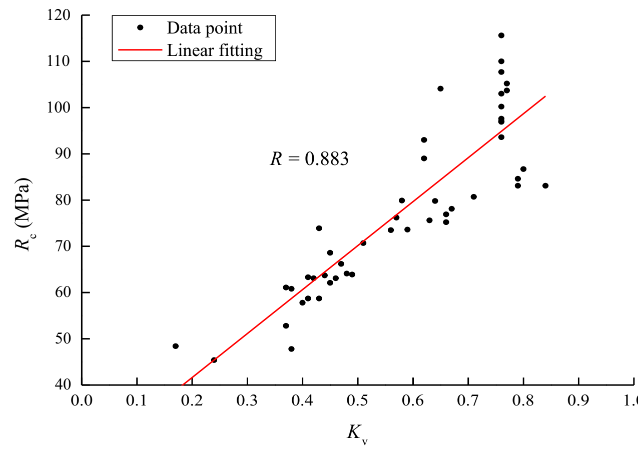

Fig. 12. Relationship between K_v and R_c.

Comparisons between the measured and predicted FPI from ridge regression, principal component regression and partial least-squares regression are shown in Figs. 13–15, respectively. As can be seen in the three figures, most of the residuals are less than 10 kN/cutter/mm/rev. In addition, it can be found that among the three models, linear fitting line of the measured and predicted FPI from the partial least-squares regression is closest to 1:1 line, meaning the optimal regression effect, and then the principal component regression and last the ridge regression. This is mainly because that the partial least-squares regression, as the second generation of regression analysis, integrates the advantages of principal component regression, canonical correlation analysis and multiple linear regression. Reliability of the principal component regression model would decrease due to that some useful independent variables would be missing easily for their relatively smaller correlation coefficients during selecting the principal components. Moreover, selection of the ridge parameter k, affected by human factor to some extent, can significantly influence the partial regression coefficients in the ridge regression model.

5. Discussion

The existing rock mass classification systems that are widely used for rock mass characterization, stability analysis and support design, such as RMR system, Q system, BQ method and HC method, were developed primarily based on the stability of surrounding

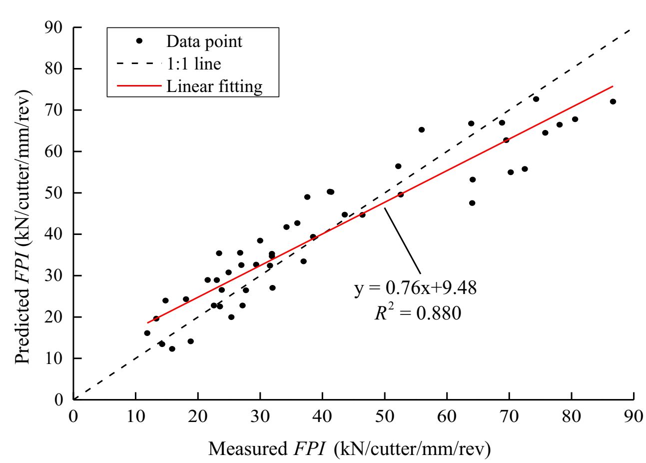

Fig. 13. Comparison between the measured and predicted FPI from ridge regression (Eq. (13)).

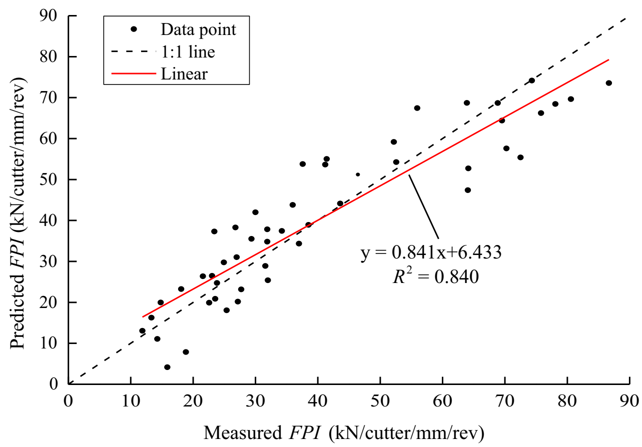

Fig. 14. Comparison between the measured and predicted *FPI* from principal component regression (Eq. (14)).

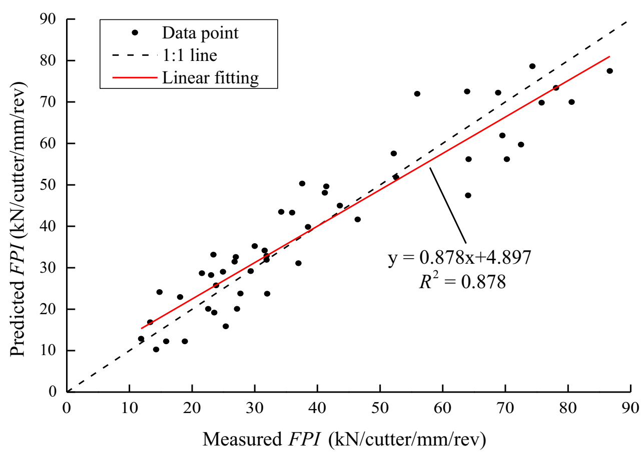

Fig. 15. Comparison between the measured and predicted *FPI* from partial least-squares regression (Eq. (15)).

rock. The desirable results for TBM performance prediction cannot be obtained by using the ratings of these rock mass classification systems mandatorily. This is mainly because that, On the one hand, the influence parameters of rock mass boreability are somewhat different from the ones controlling the stability of surrounding rock; on the other hand, the ratings assigned to the input parameters of these rock mass classification systems are not suitable for evaluating rock mass boreability. As stated by Hamidi et al. (2011): "these existing rock mass classification systems with limited accuracy in TBM performance prediction were designed with special weighting system for each rating factor for use in ground support design and not mindful of their influence on TBM performance". Therefore, only by selecting the proper rock mass parameters that mainly control rock mass boreability and assigning reasonable weight to each of them, then a rock mass classification system applicable for evaluating rock mass boreability in TBM tunnelling can be developed. Barton (1999), Bieniawski et al. (2006, 2007a, 2007b, 2008) and Bieniawski and Grandori (2007) have carried out several investigation and research on this topic.

FPI, eliminating the influence of total thrust of hydro-cylinder, shield friction force, penetration per revolution and cutter ring number, is employed for evaluating rock mass boreability in this study, yet some machine parameters, e.g. cutter diameter, cutter spacing and cutter tip width, are not taken into account in the developed models. It can be found from Figs. 13–15 that when the measured *FPI* values are relatively high, the residual error between the measured and prediction *FPI* will increase. This may be related to that the influence of rock brittleness on *FPI* is not considered in the developed models. Because that higher measured *FPI* usually indicates higher rock strength and brittleness (see Fig. 3 (a)), and rock brittleness can dramatically affect the size and shape of the crushed zone and the number and length of the cracks in rock cutting process, and then affects TBM performance (Gong and Zhao, 2007). Besides, the influences of other intact rock properties on *FPI*, e.g. rock type, abrasiveness and grain size, are not included in the developed models.

Empirical TBM performance prediction models are usually developed based on special databases with certain input parameter ranges, thus unreliable prediction results would be obtained beyond the corresponding application scope. The original datasets used for developing empirical models in this study were collected from a water conveyance tunnel mostly excavated in medium to hard igneous rocks. Therefore, it is suggested that the new proposed model for TBM performance prediction is only applicable for similar ground conditions.

Farrokh et al. (2012) strongly recommended the use combination of models to ensure a higher degree of confidence in the development of final estimates for most of the existing models tend to overestimate TBM performance, which highlights the complexity of TBM performance prediction and the powerful challenge encountered in the tunnel industry. The results in this study are beneficial explorations for estimating TBM performance in China. The input parameters for developing empirical models show clear multicollinearity in this study, but the degree of multicollinearity between the independent variables is closely related to the sample number in the database, and thus more sample datasets can effectively reduce the multicollinearity degree. Therefore, more field data from different projects need to be collected to extend the models developed in this study, and a universal model applicable for the varying ground conditions and machine types will be developed in the future. It deserves to mention that in order to guarantee the stability of the coefficient estimation, the sample number in the database should be preferred more than 20 times of the number of the independent variables, and the problem of insufficient inspection efficiency will occur when the sample number is less than the suggested value. In the latter case, the conclusion with statistically significance is still credible, but one needs to keep in mind that the coefficient estimation may be unstable (Zhang and Dong, 2013).

6. Conclusions

TBMs are being more and more widely employed in excavating tunnels in China, however, the progress of developing TBM performance prediction models is relatively slow with only two simple empirical models are established by Chinese researchers. The input parameters of RMR or Q system are quite different with those used in BQ or HC method, the two commonly used rock mass classification methods in China, which indirectly limits the applicability of the foreign developed TBM performance prediction models for the China's TBM tunnelling projects. Therefore, by employing a multiple regression analysis method on 49 field datasets collected from a 5.234 km long water conveyance tunnel mostly excavated in medium to hard igneous rocks, an attempt was made to establish an empirical model for hard rock TBM performance prediction by using HC method. The following conclusions are supported in this study:

(1) TBM penetration rate reaches its maximum value in the *HC* range 40–60 and *BQ* range 350–450, respectively. *FPI* of the rock mass in class III is lower than that in class II, which

implies that rock mass boreability of the former is higher than that of the latter. *FPI* remains nearly unchanged for the rock mass in class IV.

(2) Among all the input parameters of HC method, uniaxial compressive strength of intact saturated rock and intactness index of rock mass are significantly related to *FPI*, and discontinuity conditions, groundwater condition and attitude of the major discontinuity plane are meaninglessly correlated with *FPI*, thus the latter three parameters are excluded from the set of independent variables in regression analysis. Meanwhile, the angle between the discontinuity plane and tunnel axis and average overburden of tunnel section are also related to *FPI* to some extent. Besides, the assigned weights for the input parameters of HC method is also not suitable for evaluating rock mass boreability in TBM tunneling, therefore, the prediction accuracies of TBM performance based on *HC* or *BQ* are very limited.

(3) Ridge regression, principal component regression and partial least-squares regression methods were employed to solve the multicollinearity between uniaxial compressive strength of intact saturated rock, intactness index of rock mass, angle between the discontinuity plane and tunnel axis, and average overburden of tunnel section. Comparisons between the measured and predicted *FPI* based on the above three methods show good agreement. This highlights the powerful potential of multiple regression model based on HC method in TBM performance prediction.

(4) The empirical relationships developed in this study should be considered valid only in new projects with geological conditions similar to the studied tunnel in this study. The optimum application ranges of each parameter of the proposed formulas are summarized as follows: $45 \le R_c \le 115$ MPa; $0.15 \le K_v \le 0.85$; $18° \le \alpha \le 77°$ and $110 \le H \le 400$ m. In addition, more field data from different projects need to be collected to extend the models developed in this study, and a universal model applicable for the varying ground conditions and machine types will be developed in the future.

Acknowledgments

The authors would like to thank Dong Silong of China Railway Tunnel Group Company Limited for helping in the collection of field data and thank the funds provided by China National Key Basic Research Program under Grant Nos. 2014CB046904 and 2015CB058102, Key Program of National Natural Science Foundation of China under Grant No. 41130742 and National Funded Program for Graduate Students Studying Abroad of China Scholarship Council under Grant No. 201506270068 (to Miss Xiaoxuan Kong). Besides, the authors are also grateful to the anonymous reviewers for their careful reading of our manuscript and their many helpful comments.

References

Aeberli, U., Wanner, W.J., 1978. On the influence of discontinuities at the application of tunnelling machines. In: Proceedings of the 3rd International Congress IAEG, Madrid, pp. 7–14.

Alber, M., 2000. Advance rates of hard rock TBMs and their effects on project economics. Tunn. Undergr. Space Technol. 15 (1), 55–64. http://dx.doi.org/10.1016/S0886-7798(00)00029-8.

Alvarez Grima, M., Bruines, P.A., Verhoef, P.N.W., 2000. Modelling tunnel boring machine performance by neuro-fuzzy methods. Tunn. Undergr. Space Technol. 15 (3), 259–269. http://dx.doi.org/10.1016/S0886-7798(00)00055-9.

Bamford, W.F., 1984. Rock test indices are being successfully correlated with tunnel boring machine performance. Proceedings of the 5th Australian Tunnelling Conference, Melbourne, vol. 2, pp. 9–22.

Barton, N., Lien, R., Lunde, J., 1974. Engineering classification of rock masses for the design of tunnel support. Rock Mech. 6 (4), 189–236. http://dx.doi.org/10.1007/BF01239496.

Barton, N., 1999. TBM performance in rock using Q_{TBM}. Tunnels Tunn. Int. 31, 41–48.

Bejari, H., Hamidi, J.K., 2013. Simultaneous effects of joint spacing and orientation on TBM cutting efficiency in jointed rock masses. Rock Mech. Rock Eng. 46 (4), 897–907. http://dx.doi.org/10.1007/s00603-012-0314-2.

Bieniawski, Z.T., 1989. Engineering Rock Mass Classifications. John Wiley & Sons, New York, p. 251.

Bieniawski, Z.T., Tamames, B.C., Fernandez, J.M.G., Hernandez, M.A., 2006. Rock Mass Excavability (RME) Indicator: new way to selecting the optimum tunnel construction method. In: ITA-AITES World Tunnel Congress & 32nd ITA General Assembly, Seoul.

Bieniawski, Z.T., Celada, B., Galera, J.M., 2007a. TBM excavability: prediction and machine-rock interaction. In: Proceedings of Rapid Excavation and Tunnelling Conference, Toronto, pp. 1118–1130.

Bieniawski, Z.T., Celada, B., Galera, J.M., 2007b. Predicting TBM excavability. Tunnels Tunn. Int. (September), 25–28.

Bieniawski, Z.T., Grandori, R., 2007. Predicting TBM excavability – part II. Tunnels Tunn. Int. (December), 15–18.

Bieniawski, Z.T., Celada, B., Galera, J.M., Tardáguila, I., 2008. New applications of the excavability index for selection of TBM types and predicting their performance. In: Proceedings of the World Tunnel Congress, Agra, pp. 1618–1629.

Blindheim, O.T., 1979. Boreability Predictions for Tunnelling Ph.D. Thesis. The Norwegian Institute of Technology, Norway, p. 406.

Bruland, A., 1998. Hard Rock Tunnel Boring Ph.D. Thesis. Norwegian University of Science and Technology, Trondheim, Norway.

Cassinelli, F., Cina, S., Innaurato, N., Mancini, R., Sampaolo, A., 1982. Power consumption and metal wear in tunnel-boring machines: analysis of tunnel-boring operation in hard rock. In: Tunnelling 82, London. Inst. Min. Metall., pp. 73–81.

Chen, L.H., Labuz, J.F., 2006. Indentation of rock by wedge-shaped tools. Int. J. Rock Mech. Min. Sci. 43 (7), 1023–1033. http://dx.doi.org/10.1016/j.ijrmms.2006.03.005.

Delisio, A., Zhao, J., Einstein, H.H., 2013. Analysis and prediction of TBM performance in blocky rock conditions at the Lötschberg base tunnel. Tunn. Undergr. Space Technol. 33, 131–142. http://dx.doi.org/10.1016/j.tust.2012.06.015.

Delisio, A., Zhao, J., 2014. A new model for TBM performance prediction in blocky rock conditions. Tunn. Undergr. Space Technol. 43, 440–452. http://dx.doi.org/10.1016/j.tust.2014.06.004.

Du, L.J., Qi, Z.C., Han, X.L., Zhou, J.F., Chen, Z.W., Du, Y.L., 2015. Prediction method for the boreability and performance of hard rock TBM based on jobsite boring data. J. Chin. Coal Soc. 40 (6), 1284–1289. http://dx.doi.org/10.13225/j.cnki.jccs.2014.3035 (in Chinese).

Farmer, I.W., Glossop, N.H., 1980. Mechanics of disc cutter penetration. Tunnels Tunn. Int. 12 (6), 22–25.

Farrokh, E., Rostami, J., Laughton, C., 2012. Study of various models for estimation of penetration rate of hard rock TBMs. Tunn. Undergr. Space Technol. 30, 110–123. http://dx.doi.org/10.1016/j.tust.2012.02.012.

Franklin, J.A., 1979. Suggested methods for determining water content, porosity, density, absorption and related properties. Int. J. Rock Mech. Min. Sci. 16 (2), 143–151.

Franklin, J.A., 1985. Suggested method for determining point load strength. Int. J. Rock Mech. Min. Sci. Geomech. Abstr. 22 (2), 51–60. http://dx.doi.org/10.1016/0148-9062(85)92327-7.

Gong, Q.M., Zhao, J., Jiao, Y.Y., 2005. Numerical modeling of the effects of joint orientation on rock fragmentation by TBM cutters. Tunn. Undergr. Space Technol. 20 (2), 183–191. http://dx.doi.org/10.1016/j.tust.2004.08.006.

Gong, Q.M., Zhao, J., Jiang, Y.S., 2007. In situ TBM penetration tests and rock mass boreability analysis in hard rock tunnels. Tunn. Undergr. Space Technol. 22 (3), 303–316. http://dx.doi.org/10.1016/j.tust.2006.07.003.

Gong, Q.M., Zhao, J., 2007. Influence of rock brittleness on TBM penetration rate in Singapore granite. Tunn. Undergr. Space Technol. 22 (3), 317–324. http://dx.doi.org/10.1016/j.tust.2006.07.004.

Gong, Q.M., Zhao, J., 2009. Development of a rock mass characteristics model for TBM penetration rate prediction. Int. J. Rock Mech. Min. Sci. 46 (1), 8–18. http://dx.doi.org/10.1016/j.ijrmms.2008.03.003.

Gong, Q.M., She, Q.R., Hou, Z.S., Jiang, H.T., Peng, Q., 2010. Experimental study of TBM penetration in marble rock mass under high geostress. Chin. J. Rock Mech. Eng. 29 (12), 2522–2532 (in Chinese).

Gong, Q.M., Yin, L.J., Wu, S.Y., Zhao, J., Ting, Y., 2012. Rock burst and slabbing failure and its influence on TBM excavation at headrace tunnels in Jinping II hydropower station. Eng. Geol. 124, 98–108. http://dx.doi.org/10.1016/j.enggeo.2011.10.007.

Graham, P.C., 1976. Rock exploration for machine manufacturers. Explor. Rock Eng., 173–180

Grandori, R., Sem, M., Lembo-Fazio, A., Ribacchi, R., 1995. Tunnelling by double shield TBM in the Hong Kong granite. Proceedings of the 8th ISRM Congress, Rotterdam, vol. 1, pp. 569–574.

Hamidi, J.K., Shahriar, K., Rezai, B., Rostami, J., 2010. Performance prediction of hard rock TBM using Rock Mass Rating (RMR) system. Tunn. Undergr. Space Technol. 25 (4), 333–345. http://dx.doi.org/10.1016/j.tust.2010.01.008.

Hamidi, J.K., Shahriar, K., Rezai, B., Rostami, J., 2011. Response by the authors to S. Yagiz discussion to the paper: J. Khademi Hamidi et al., Performance prediction of hard rock TBM using Rock Mass Rating (RMR) system [Tunnell. Undergr.

Space Technol. 25 (2010) 333–345]. Tunn. Undergr. Space Technol. 26 (6), 795–797. http://dx.doi.org/10.1016/j.tust.2011.05.012.
Hamilton, W.H., Dollinger, G.L., 1979. Optimizing tunnel boring machine and cutter design for greater boreability. In: Proceedings of the Rapid Excavation and Tunnelling Conference, Atlanta, pp. 280–296.
Hassanpour, J., Rostami, J., Khamehchiyan, M., Bruland, A., 2009. Developing new equations for TBM performance prediction in carbonate-argillaceous rocks: a case history of Nowsood water conveyance tunnel. Geomech. Geoeng. Int. J. 4 (4), 287–297. http://dx.doi.org/10.1080/17486020903174303.
Hassanpour, J., Rostami, J., Khamehchiyan, M., Bruland, A., Tavakoli, H.R., 2010. TBM performance analysis in pyroclastic rocks: a case history of Karaj water conveyance tunnel. Rock Mech. Rock Eng. 43 (4), 427–445. http://dx.doi.org/10.1007/s00603-009-0060-2.
Hassanpour, J., Rostami, J., Zhao, J., 2011. A new hard rock TBM performance prediction model for project planning. Tunn. Undergr. Space Technol. 26 (5), 595–603. http://dx.doi.org/10.1016/j.tust.2011.04.004.
Hoek, E., Brown, E.T., 1997. Practical estimates of rock mass strength. Int. J. Rock Mech. Min. Sci. 34 (8), 1165–1186. http://dx.doi.org/10.1016/S1365-1609(97)80069-X.
Huang, H., Damjanac, B., Detournay, E., 1998. Normal wedge indentation in rocks with lateral confinement. Rock Mech. Rock Eng. 31 (2), 81–94. http://dx.doi.org/10.1007/s006030050010.
Hughes, H.M., 1986. The relative cuttability of coal-measures stone. Min. Sci. Technol. 3 (2), 95–109. http://dx.doi.org/10.1016/S0167-9031(86)90250-1.
Innaurato, N., Mancini, R., Rondena, E., Zaninetti, A., 1991. Forecasting and effective TBM performances in a rapid excavation of a tunnel in Italy. In: Proceedings of the 7th International Congress ISRM, Aachen, pp. 1009–1014.
Innaurato, N., Oggeri, C., Oreste, P.P., Vinai, R., 2007. Experimental and numerical studies on rock breaking with TBM tools under high stress confinement. Rock Mech. Rock Eng. 40 (5), 429–451. http://dx.doi.org/10.1007/s00603-006-0109-4.
Kaitkay, P., Lei, S.T., 2005. Experimental study of rock cutting under external hydrostatic pressure. J. Mat. Proc. Technol. 159 (2), 206–213. http://dx.doi.org/10.1016/j.jmatprotec.2004.04.418.
Kong, X.X., Liu, Q.S., Zhao, Y.F., Pan, Y.C., Liu, J.P., 2015. Numerical simulation on the effect of joint orientation on rock fragmentation by TBM disc cutters. J. Chin. Coal Soc. 40 (6), 1257–1262. http://dx.doi.org/10.13225/j.cnki.jccs.2014.3038 (in Chinese).
Laughton, C., 1998. Evaluation and Prediction of Tunnel Boring Machine Performance in Variable Rock Masses Ph.D. Thesis. The University of Texas, Austin, USA.
Lislerud, A., 1988. Hard rock tunnel boring: prognosis and cost. Tunn. Undergr. Space Technol. 3 (1), 9–17. http://dx.doi.org/10.1016/0886-7798(88)90029-6.
Liu, Q.S., Huang, X., Gong, Q.M., Du, L.J., Pan, Y.C., Liu, J.P., 2016a. Application and development of hard rock TBM and its prospect in China. Tunn. Undergr. Space Technol. 57, 1–14. http://dx.doi.org/10.1016/j.tust.2016.01.034.
Liu, Q.S., Liu, J.P., Pan, Y.C., Kong, X.X., Cui, X.Z., Huang, S.B., Wei, L., 2016b. Research advances of tunnel boring machine (TBM) performance prediction models for hard rock. Chin. J. Rock Mech. Eng. 35 (Suppl. 1), 865–876. http://dx.doi.org/10.13722/j.cnki.jrme.2014.1601 (in Chinese).
Ma, H.S., Ji, H.G., 2011. Experimental study of the effect of joint orientation on fragmentation modes and penetration rate under TBM disc cutters. Chin. J. Rock Mech. Eng. 30 (1), 155–163 (in Chinese).
Ma, H.S., Yin, L.J., Ji, H.G., 2011. Numerical study of the effect of confining stress on rock fragmentation by TBM cutters. Int. J. Rock Mech. Min. Sci. 48 (6), 1021–1033. http://dx.doi.org/10.1016/j.ijrmms.2011.05.002.
McFeat-Smith, I., Askilsrud, O.G., 1993. Tunnel boring machines in Hong Kong. In: Proceedings, Rapid Excavation and Tunnelling Conference, Boston, pp. 401–413.
Mo, Z.Z., Li, H.B., Zhou, Q.C., He, E.G., Zou, F., Zhu, X.M., Zhao, Y., 2012. Research on numerical simulation of rock breaking using TBM disc cutters based on UDEC method. Rock Soil Mech. 33 (4), 1196–1202 (in Chinese).
Nelson, P., O'Rourke, T.D., Kulhawy, F.H., 1983. Factors affecting TBM penetration rates in sedimentary rocks. In: Proceedings of 24th US Symposium on Rock Mechanics, Texas A&M, pp. 227–237.
Nelson, P., Ingraffea, A.R., O'Rouke, T.D., 1985. TBM performance prediction using rock fracture parameters. Int. J. Rock Mech. Min. Sci. Geomech. Abstr. 22 (3), 189–192. http://dx.doi.org/10.1016/0148-9062(85)93234-6.
Palmström, A., 1995. RMi – A Rock Mass Characterization System for Rock Engineering Purposes Ph.D. Thesis. University of Oslo, Oslo, Norway, p. 400.
Paltrinieri, E., Sandrone, F., Zhao, J., 2016. Analysis and estimation of gripper TBM performances in highly fractured and faulted rocks. Tunn. Undergr. Space Technol. 52, 44–61. http://dx.doi.org/10.1016/j.tust.2015.11.017.
Pelizza, S., Grasso, P., Xu, S.L., Di, J.Y., 2002. Review of TBM tunnelling. Constr. Mach. 5, 21–27 (in Chinese).
Qian, Q.H., Li, C.P., 2002. The present and prospect of application of tunneler in China's underground engineering. Undergr. Space 22, 1–11 (in Chinese).
Ramezanzadeh, A., 2005. Performance Analysis and Development of New Models for Performance Prediction Of Hard Rock TBMs in Rock Mass Ph.D. Thesis. INSA de Lyon, France, p. 333.
Reilly, J., Arrigoni, G., Xu, S.L., Grasso, P., 2002. TBM and its applications in China. Mod. Tunn. Technol. 39 (3), 1–6 (in Chinese).
Ribacchi, R., Lembo-Fazio, A., 2005. Influence of rock mass parameters on the performance of a TBM in a gneissic formation (Varzo Tunnel). Rock Mech. Rock Eng. 38 (2), 105–127. http://dx.doi.org/10.1007/s00603-004-0032-5.
Rostami, J., Ozdemir, L., 1993. A new model for performance prediction of hard rock TBM. In: Proceedings of Rapid Excavation and Tunnelling Conference, pp. 793–809.
Rostami, J., Ozdemir, L., Nilsen, B., 1996. Comparison between CSM and NTH hard rock TBM performance prediction models. In: Proceedings of the Annual Conference of the Institution of Shaft Drilling Technology (ISDT), Las Vegas, p. 11.
Rostami, J., 1997. Development of a Force Estimation Model for Rock Fragmentation with Disc Cutters through Theoretical Modeling and Physical Measurement of Crushed Zone Pressure Ph.D. Thesis. Colorado School of Mines, Golden, Colorado, USA, p. 249.
Roxborough, F.F., Phillips, H.R., 1975. Rock excavation by disc cutter. Int. J. Rock Mech. Min. Sci. Geomech. Abstr. 12 (12), 361–366. http://dx.doi.org/10.1016/0148-9062(75)90547-1.
Sanio, H.P., 1985. Prediction of the performance of disc cutters in anisotropic rock. Int. J. Rock Mech. Min. Sci. Geomech. Abstr. 22 (3), 153–161. http://dx.doi.org/10.1016/0148-9062(85)93229-2.
Sapigni, M., Berti, M., Behtaz, E., Busillo, A., Cardone, G., 2002. TBM performance estimation using rock mass classification. Int. J. Rock Mech. Min. Sci. 39 (6), 771–788. http://dx.doi.org/10.1016/S1365-1609(02)00069-2.
Shahriar, K., Rostami, J., Khademi Hamidi, J., 2009. TBM tunnelling and analysis of high gas emission accident in Zagros long tunnel. In: Proceedings of the ITA-AITES World Tunnel Congress & 35th ITA General Assembly, Budapest, Hungary.
Shen, Y.J., Xu, G.L., Song, S.W., Li, Z.P., Feng, X.M., Dong, J.X., 2014. A classification method of surrounding rock mass in hydropower project in high geostress area. Chin. J. Rock Mech. Eng. 33 (11), 2267–2275. http://dx.doi.org/10.13722/j.cnki.jrme.2014.11.011 (in Chinese).
Snowdon, R.A., Ryley, M.D., Temporal, J., 1982. A study of disc cutting in selected British rocks. Int. J. Rock Mech. Min. Sci. Geomech. Abstr. 19 (3), 107–121. http://dx.doi.org/10.1016/0148-9062(82)91151-2.
Song, K.Z., Sun, S.X., Yuan, D.J., Wang, M.S., 2008. Fuzzy recognition for rock cuttability based on shield driving parameters. Chin. J. Rock Mech. Eng. 27 (Suppl. 1), 3196–3202 (in Chinese).
Steingrimsson, J.H., Grov, E., Nilsen, B., 2002. The significance of mixed-face conditions for TBM performance. World Tunn. 9, 435–441.
Sundaram, N.M., Rafek, A.G., 1998. The influence of rock mass properties in the assessment of TBM performance. In: Proceedings of the 8th IAEG Congress, Vancouver, pp. 3553–3559.
Sundin, N.O., Wänstedt, S., 1994. A boreability model for TBM's, In: Proceedings of the 1st North American Rock Mechanics Symposium, Rotterdam, 311–318.
Tan, Q., Zhu, Y., Xi, Y.M., Xu, Z.J., Li, J.F., Song, J.H., 2013. Influence of joint characteristics on rock fragmentation induced by TBM disc cutter. J. Central South Univ. (Sci. Technol.) 44 (10), 4040–4046 (in Chinese).
Tarkoy, P.J., 1973. Predicting TBM penetration rates in selected rock types. In: Proceedings of 9th Canadian Rock Mechanics Symposium, Montreal, pp. 263–274.
The National Standards Compilation Group of People's Republic of China, 2009. GB50487–2008 Code for Engineering Geological Investigation of Water Resources and Hydropower. China Planning Press, Beijing, p. 262 (in Chinese).
The National Standards Compilation Group of People's Republic of China, 2014. GB/T50218–2014 Standard for Engineering Classification of Rock Masses. China Planning Press, Beijing, p. 84 (in Chinese).
Tóth, Á., Gong, Q.M., Zhao, J., 2013. Case studies of TBM tunnelling performance in rock–soil interface mixed ground. Tunn. Undergr. Space Technol. 38, 140–150. http://dx.doi.org/10.1016/j.tust.2013.06.001.
Wanner, H., Aeberli, U., 1979. Tunnelling machine performance in jointed rock. In: Proceedings of 4th Congress of the International Society for Rock Mechanics, Montreux, pp. 573–580.
Wang, H.W., 1999. Partial Least-Squares Regression-Method and Applications. National Defense Industry Press, Beijing, p. 274.
Wijk, G., 1992. A model of tunnel boring machine performance. Geotech. Geol. Eng. 10 (1), 19–40. http://dx.doi.org/10.1007/BF00881969.
Wu, A.Q., Liu, F.Z., 2012. Advancement and application of the standard of engineering classification of rock masses. Chin. J. Rock Mech. Eng. 31 (8), 1513–1523 (in Chinese).
Wu, S.Y., Gong, Q.M., Wang, G., Hou, Z.S., She, Q.R., 2010. Experimental study of slabbing failure for deepburied marble at JinPing II hydropower station and its influences on TBM excavation. Chin. J. Rock Mech. Eng. 29 (6), 1089–1095 (in Chinese).
Yagiz, S., 2008. Utilizing rock mass properties for predicting TBM performance in hard rock condition. Tunn. Undergr. Space Technol. 23 (3), 326–339. http://dx.doi.org/10.1016/j.tust.2007.04.011.
Yin, L.J., Gong, Q.M., Ma, H.S., Zhao, J., Zhao, X.B., 2014. Use of indentation tests to study the influence of confining stress on rock fragmentation by a TBM cutter. Int. J. Rock Mech. Min. Sci. 72, 261–276. http://dx.doi.org/10.1016/j.ijrmms.2014.07.022.
Zhang, W.T., Dong, W., 2013. Advanced Tutorials of Statistical Analysis with SPSS, second ed. Higher Education Press, Beijing, p. 451.
Zhao, J., Gong, Q.M., Eisensten, Z., 2007. Tunnelling through a frequently changing and mixed ground: a case history in Singapore. Tunn. Undergr. Space Technol. 22 (4), 388–400. http://dx.doi.org/10.1016/j.tust.2006.10.002.
Zou, F., Li, H.B., Zhou, Q.C., Mo, Z.Z., Zhu, X.M., Niu, L., Yang, F.W., 2012. Experimental study of influence of joint space and joint angle on rock fragmentation by TBM disc cutter. Rock Soil Mech. 33 (6), 1640–1646 (in Chinese).